J Mater Sci (2008) 43:4182–4191
DOI 10.1007/s10853-008-2598-x

Poly(thiophenylanilino) and poly(furanylanilino) polymers

Lawrence C. Baldwin · Andrew P. Chafin · Jeffrey R. Deschamps · Samantha A. Hawkins · Michael E. Wright · David L. Witker · Nicholas Prokopuk

Received: 5 September 2007 / Accepted: 14 March 2008 / Published online: 23 April 2008

Abstract Novel hybrid polymers with thiophenylanilino and furanylanilino backbones and substituted phenyl side groups are reported. The new monomers bis-(4-heterocyclic-2-yl-phenyl)-aryl-amine (heterocyclic = thiophen with aryl = 4-benzoyl (**2a**), 4-nitro-phenyl (**2b**) and furan with aryl = 4-benzoyl-phenyl (**3a**), 4-nitro-phenyl (**3b**)) were prepared by monosubstituting triphenylamine under electrophilic aromatic conditions affording 4-nitrotriphenylamine and 4-benzoyltriphenylamine. Di(bromination) of the latter compounds followed by Stille cross-coupling reactions with 2-tributylstannylthiophene or 2-tributylstannylfuran produces the new monomers **2a–b** and **3a–b** in high yield. The monomers are electrochemically polymerized at relatively low potentials (<0.8 V versus $Ag^+/AgCl$) in acetonitrile electrolytes resulting in electroactive films. All the new polymers can be repeatedly oxidized and reduced with little loss of electrochemical activity. Vibrational spectroscopy reveals that the monomer units are connected predominately via coupling of the thiophenyl or furanyl rings yielding the novel polymers. Single-crystal molecular structure determinations of 4-nitrotriphenylamine and monomer **3b** indicate the importance of the electron-withdrawing groups on the pendent phenyl groups in determining the extent of delocalization of the extended multi-ring systems. Molecular orbital calculations suggest that the HOMO of **2b** is delocalized about both anilino and thiophenyl portions of the molecule.

Electronic supplementary material Supplementary material is available for this article at 10.1007/s10853-008-2598-x and is accessible for authorized users.

L. C. Baldwin · A. P. Chafin · S. A. Hawkins · M. E. Wright · D. L. Witker · N. Prokopuk (✉)
Research & Science Engineering Department, Research Division, Chemistry Branch, NAVAIR, China Lake, CA 93555-6100, USA
e-mail: nicholas.prokopuk@navy.mil

J. R. Deschamps
Naval Research Laboratory, Code 6030 4555 Overlook Ave., Washington, DC 20375, USA

Introduction

Conjugated organic polymers that exhibit reversible oxidation events are finding use in a variety of photonic [1–3] and electronic devices [4–6]. Specific applications targeted for conjugated polymers include electrode materials in light weight batteries [7, 8] and organic supercapitors [9–12], charge-transport layers in OLEDs [13, 14], photoanodes and cathodes in photovoltaic devices [15, 16], and refractive films in nonlinear optics [17]. By oxidizing or reducing the polymer backbone, the electrical and optical properties of the polymer can be tuned for optimal device performance. Furthermore, the availability of side groups provides chemical control over the polymer's physical properties.

Polyaniline derivatives are exceptionally promising materials for device applications due to the near metallic conductivity, the high stability of the doped forms to air and moisture, and low cost [7]. The related triarylamines exhibit exceptionally high photoconductivities and hole-mobilities and can form extremely stable radical cations [13]. Theoretical studies suggest that triarylamines may exhibit similarly high conductivities as polyaniline [18]. The third aryl moiety on the nitrogen stabilizes the radical by providing additional delocalization [13]. The pendent aryl also provides a straightforward approach for tuning the electronic properties of the polymer backbone by providing substitution sites for introducing electron-donating and electron-withdrawing groups. However, linear poly(triarylamines) are significantly more difficult to generate than the analogous

poly(aniline). The presence of multiple coupling sites leads to an extensively cross-linked material and the afore-mentioned stability of the radical cation slows the polymerization process. Instead, the triarylamine is often incorporated into the polymer material by tethering to the polymer backbone, attaching to end groups, or as part of the back bone through chemical coupling reactions [19–21]. Herein, we report the synthesis on the new monomers bis-(4-heterocyclic-2-yl-phenyl)-aryl-amine (heterocyclic = thiophen with aryl = 4-benzoyl (**2a**), 4-nitrophenyl (**2b**) and furan with aryl = 4-benzoyl-phenyl (**3a**), 4-nitro-phenyl (**3b**)) which undergo electrochemical polymerization at the pendent heterocycles. The resulting copolymers contain the functionalized triarylamine within the backbone. The electrochemical properties of the novel polymers are also described.

Experimental section

General methods

All manipulations of compounds and solvents were carried out using standard Schlenk techniques. Tetrahydrofuran (THF), ether, N-methylpyrrolidinone (99.5%), and dichloromethane solvents were purchased as the anhydrous grade and inhibitor-free from Aldrich and used as received. ^{1}H and ^{13}C NMR measurements were performed using a Bruker Avance 400 MHz instrument. ^{1}H and ^{13}C NMR chemical shifts are reported versus the deuterated solvent peak (Solvent, ^{1}H, ^{13}C: $CDCl_3$, δ 7.26 ppm, δ 77.2 ppm; DMSO-d_6, δ 2.50 ppm, δ 39.5 ppm). Triphenylamine, diethylaluminum chloride (1.8 M in toluene), benzoyl chloride (98%), 2-tributylstannylthiophene, and 2-tributylstannylfuran were purchased from Aldrich Chemical Co. and used as received. Diffuse reflection infrared spectroscopic measurements were acquired with a Thermo Nexus 870 spectrometer equipped with a liquid nitrogen-cooled MCTA or DTGS detector. Elemental analyses were performed at Atlantc Microlab, Inc., Norcross, GA. Molecular weight data is reported relative to polystyrene standards. Data were collected on a Viscotek model 302 HPLC using two consecutive 300 mm PL mixed-bed GPC/SEC columns with chloroform as the eluent. The nitration of triphenylamine was carried out using typical nitration conditions for activated aromatic compounds [22]. An alternative synthesis of 4-nitro-bis(4'-bromophenyl)amine has been reported by treatment of tris(4-bromophenyl)amine with tetranitromethane via a nitro-debromination reaction [23].

Friedel-Crafts benzoylation of triphenylamine

A chilled (0 °C) dichloromethane (100 mL) solution containing triphenylamine (10.00 g, 40.8 mmol) and benzoyl chloride (41 mmol) was treated dropwise with diethylaluminum chloride (22 mL, ~40 mmol). After addition was complete the mixture was allowed to react at 0 °C for 4 h with stirring. The mixture was carefully diluted with water (50 mL) and allowed to stir for 2 h. A saturated solution of sodium bicarbonate was added and the organic layer separated and then dried over $MgSO_4$. The solvent was removed under reduced pressure and the crude product was purified by column chromatography on silica gel using chloroform as the eluent.

General procedure for bromination

A chilled (0 °C) dichloromethane (100 mL) solution containing 4-(diphenylamino)benzophenone or 4-nitrotriphenylamine (~22.6 mmol) was treated dropwise with bromine (~50 mmol). After allowing the mixture to react at 0 °C for 2 h with stirring, the mixture was diluted with saturated sodium bicarbonate (50 mL). The mixture was placed in a separatory funnel and the organic layer isolated and washed with water (100 mL), brine (50 mL), and then dried over $MgSO_4$. The solvent was removed under reduced pressure and the crude product was recrystallized from ethanol to afford analytically pure **1b**. In a similar manner compound **1a** was prepared using a dilute solution of nitric acid in acetic acid for deliverance of the electrophile (i.e., NO_2).

General procedure for the Stille cross-coupling of the bis-(4-bromo-phenyl)-(4-X-phenyl)-amine (where X = benzoyl or nitro) with the 2-(tributylstannyl)thiophene (to afford **2a** and **2b**, respectively) and 2-tributylstannylfuran (to afford **3a** and **3b**, respectively)

A Schlenk flask was charged with the appropriate dibromotriarylamine (10 mmol), organostannane reagent (20 mmol), $(PPh_3)_2PdCl_2$ (0.5 mmol), and DMF (25 mL). The mixture was heated at 50 °C for 24 h with stirring and then diluted with chloroform and washed with water (5 × 100 mL). The solvent was removed under reduced pressure and crude product was subjected to chromatography on silica gel (chloroform/hexanes, 8/2, v/v). The major band was collected and the solvents removed under reduced pressure. The solid was recrystallized by diffusing pentane into a chloroform or acetone solution of the product. Solvent co-crystallization occurs for both acetone and chloroform.

Spectroscopic data for **2a**: ^{1}H NMR (400 MHz, $CDCl_3$): 7.80 (d, J = 7.4 Hz, *H*15, 2H), 7.75 (d, J = 8.8 Hz, *H*3, 2H), 7.58 (d, J = 8.4 Hz, *H*7, 4H), 7.60-7.50 (m, *H*17, 1H), 7.48 (t, J = 7.4 Hz, *H*16, 2H), 7.29-7.26 (m, *H*12 and *H*10, 4H), 7.19 (d, J = 8.4 Hz, *H*6, 4H), 7.12 (d, J = 8.8 Hz, *H*2, 2H), 7.09 (dd, J = 5.0 and 3.8 Hz, *H*11, 2H); ^{13}C NMR (100 MHz, $CDCl_3$): 195.3 (*C*13), 151.5 (*C*1), 145.8 (*C*5), 143.9 (*C*9), 138.6 (*C*14), 132.2 (C3), 132.0 (*C*17), 131.0 (*C*8), 130.7 (*C*4), 129.9 (*C*15), 128.4 (*C*11), 128.3

(*C*16), 127.3 (*C*7), 126.1 (*C*6), 124.9 (*C*12 or *C*10), 123.1 (*C*12 or *C*10), 120.8 (*C*2). Yield is 50%.

Spectroscopic data for **2b**:^{1}H NMR (400 MHz, $CDCl_3$) δ 8.08 (d, $J = 9.3$ Hz, *H*3, 2H), 7.61 (d, $J = 8.6$ Hz, *H*9, 4H), 7.30 (m, *H*15 and *H*17, 4H), 7.19 (d, $J = 7.6$ Hz, *H*8, 4H), 7.10 (dd, $J = 5.0$ and 3.6 Hz, *H*16, 2H), 7.04 (d, $J = 9.3$ Hz, *H*2, 2H); ^{13}C NMR (100 MHz, $CDCl_3$): 152.1 (*C*1), 144.9 (*C*7), 143.5 (*C*13), 140.9 (*C*4), 132.0 (*C*10), 128.4 (*C*16), 127.5 (*C*9), 126.7 (*C*8), 125.7 (*C*3), 125.3 (*C*15 or *C*17), 123.5 (*C*15 or *C*17), 119.3 (*C*2). Yield is 47%.

Spectroscopic data for **3a**:^{1}H NMR (400 MHz, $CDCl_3$) δ 7.79 (d, $J = 7.4$ Hz, *H*15, 2H), 7.74 (d, $J = 8.6$ Hz, *H*3, 2H), 7.63 (d, $J = 8.6$ Hz, *H*7, 4H), 7.55 (t, $J = 7.4$ Hz, *H*17, 1H), 7.47 (t, $J = 7.4$ Hz, *H*16, 2H), 7.46 (d, $J = 1.7$ Hz, *H*12, 2H), 7.19 (d, $J = 8.6$ Hz, *H*6, 4H), 7.10 (d, $J = 8.6$ Hz, *H*2, 2H), 6.61 (d, $J = 3.3$ Hz, *H*10, 2H), 6.48 (dd, $J = 3.3$ and 1.7 Hz, *H*11, 2H); ^{13}C NMR (100 MHz, $CDCl_3$) δ 195.4 (*C*13), 153.8 (*C*9), 151.6 (*C*1), 145.7 (*C*5), 142.3 (*C*12), 138.6 (*C*14), 132.2 (*C*3), 132.0 (*C*17), 130.6 (*C*4), 129.9 (*C*15), 128.4 (*C*16), 127.5 (*C*8), 126.0 (*C*6), 125.3 (*C*7), 120.7 (*C*2), 111.9 (*C*11), 105.0 (*C*10). Yield is 47%.

Selected data for monomer **3b**: ^{1}H NMR (400 MHz, $CDCl_3$) δ 8.07 (d, $J = 9.3$ Hz, *H*3, 2H), 7.66 (d, $J = 8.7$ Hz, *H*9, 4H), 7.48 (m, $J = 1.8$ Hz, *H*15, 2H), 7.19 (d, $J = 8.7$ Hz, *H*8, 4H), 7.02 (d, $J = 9.3$, *H*2, 2H), 6.65 (d, $J = 3.3$ Hz, *H*17, 2H), 6.49 (dd, $J = 1.8$ and 3.3 Hz, *H*16, 2H); ^{13}C NMR (100 MHz, $CDCl_3$) δ 153.4 (*C*13), 153.2 (*C*1), 144.7 (*C*5), 142.5 (*C*15), 140.9 (*C*4), 128.5 (*C*10), 126.6 (*C*8), 125.7 (*C*3), 125.5 (*C*9), 119.3 (*C*2), 112.0 (*C*16), 105.5 (*C*17). Yield is 29%.

X-ray crystal structures of 4-nitrotriphenylamine and bis-(4-furan-2-yl-phenyl)-(4-nitro-phenyl)-amine (**3b**)

Single-crystal X-ray diffraction data on both compounds were collected at 103 K using MoKα radiation and a Bruker APEX2 CCD area detector. Corrections were applied for Lorentz, polarization, and absorption effects. The structures were solved by direct methods and refined by full-matrix least squares on F^2 values using the programs found in the SHELXTL suite (Bruker, SHELXTL v6.10, 2000, Bruker AXS Inc., Madison, WI). Parameters refined included atomic coordinates and anisotropic thermal parameters for all nonhydrogen atoms. Hydrogen atoms on carbons were included using a riding model (coordinate shifts of C applied to H atoms) with C–H distance set at 0.096 nm. Atomic coordinates for compounds 4-nitrophenylamine and **3b** have been deposited with the Cambridge Crystallographic Data Centre (deposition numbers 657298 and 657299). Copies of the data can be obtained, free of charge, on application to CCDC, 12 Union Road, Cambridge, CB2 1EZ, UK (fax: +44(0)-1223-336033 or e-mail: deposit@ccdc.cam.ac.uk).

A $0.73 \times 0.44 \times 0.39$ mm^3 crystal of 4-nitrotriphenylamine was prepared for data collection by coating with high viscosity microscope oil (Paratone-N, Hampton Research). The oil-coated crystal was mounted on a glass rod and transferred immediately to the cold stream (−170 °C) on the diffractometer. The crystal was orthorhombic in space group *P*bca with unit cell dimensions $a = 1.28372(10)$ nm, $b = 1.29064(9)$ nm, $c = 1.72640(12)$ nm. Data were 98.9% complete to 29.16° θ (approximately 0.073 nm) with an average redundancy of 4.7. The asymmetric unit contains one molecule.

A $0.53 \times 0.18 \times 0.10$ mm^3 crystal of **3b** was prepared for data collection coating with high viscosity microscope oil (Paratone-N, Hampton Research). The oil-coated crystal was mounted on a glass rod and transferred immediately to the cold stream (−170 °C) on the diffractometer. The crystal was triclinic in space group *P*-1 with unit cell dimensions $a = 1.39564(6)$ nm, $b = 1.51172(6)$ nm, $c = 2.31004(9)$ nm, $\alpha = 87.050(1)°$, $\beta = 89.978(1)°$, and $\gamma = 76.656(1)°$. Data were 99.2% complete to 25.35° θ (approximately 0.083 nm) with an average redundancy of 2.3. The asymmetric unit contains four molecules plus two molecules of cyclohexane. POLYMORPH: The crystal was monoclinic in space group *C* 2/c with unit cell dimensions $a = 2.9111(4)$ nm, $b = 0.70385(6)$ nm, $c = 2.3021(4)$ nm, $\beta = 91.410(5)°$. The asymmetric unit contains a single molecule. Both furan rings are disordered over two positions. There appears to be unresolved twinning such that significant errors are still present in the model.

Electrochemical experimental methods

Electrochemical measurements were performed with a Princeton Applied Research 273 Potentiostat/galvanostat using a conventional three-electrode configuration. A Pt-bead or -disk working electrode, Pt-mesh counter electrode, and a nonaqueous Ag/Ag^+ reference electrode were employed. Electrochemical experiments were performed in a nitrogen-purged glove box with 0.1 M tetrabutylammonium tetrafluoroborate in acetonitrile. Tetrabutylammonium tetrafluoroborate (Aldrich) was recrystallized from ethanol/diethyl ether and dried in vacuum. Acetonitrile (Aldrich) was distilled from CaH_2 under N_2 prior to use. Polymer films were grown electrochemically by cycling the potential between 0 and 1 V versus Ag/Ag^+ at 50 mV/s of a Pt-disk electrodes immersed in an electrolyte solution that is 0.1–50 mM in the monomer.

DFT calculations

All calculations were performed by the Gaussian03 program using the b3lyp DFT functional [24]. Geometries of both the neutral ground state and the radical cation were

optimized using the 6-31g(d,p) basis set and a frequency calculation performed. No imaginary frequencies were found indicating a true minimum. Single point energy calculations on the optimized geometry for both the neutral ground state and the radical cation were then performed using the 6-311++g(3df,2p) basis set. The gas phase adiabatic ionization potential (IP) was taken as the difference in energy between the ground state neutral molecule and the radical cation using the 6-311++g(3df,2p) basis set with thermal corrections to 298 °C at the 6-31g(d,p) level. Liu's correction for improving the under estimation of IPs using b3lyp is employed in addition to their procedure to calculate standard potentials in acetonitrile from gas phase IP's [43]. The vertical, adiabatic, and corrected ionization potentials are listed in Table 2.

Results and discussion

Synthesis and characterization of the monomers

The monomers **2** and **3** were prepared in an efficient three-step process starting from triphenylamine as outlined in Scheme 1. Diethylaluminum chloride is the Lewis acid of choice for electrophilic aromatic substitution on triphenylamine derivatives [25]. Several cross-coupling reaction methodologies would likely work [26]; however, the Stille reaction [27] using commercially available 2-(tributylstannyl)-thiophene and -furan is convenient and affords the desired coupled products in excellent chemical yields. The use of LiCl and a dipolar aprotic solvent like dimethylformamide greatly facilitates the Stille cross-coupling with the arylamine bromides used in this study [28, 29].

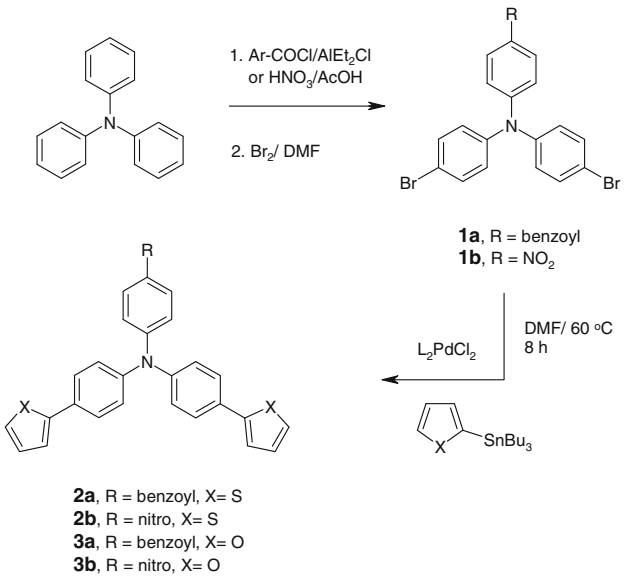

Scheme 1 Reaction scheme for synthesizing new monomers

The monomers **2** and **3** were characterized by detailed NMR spectroscopic analysis with complete assignments in the proton and carbon spectra. In selected cases single-crystal X-ray analyses was performed to obtain solid-state structural information for use in conjunction with molecular orbital calculations vida infra. The molecular structures of 4-nitrotriphenylamine and monomer **3b** reveal the expected geometry about the central nitrogen as determined by single-crystal X-ray diffraction, Figs. 1 and 2. A summary of the crystallographic data collection parameters is presented in Table 1.

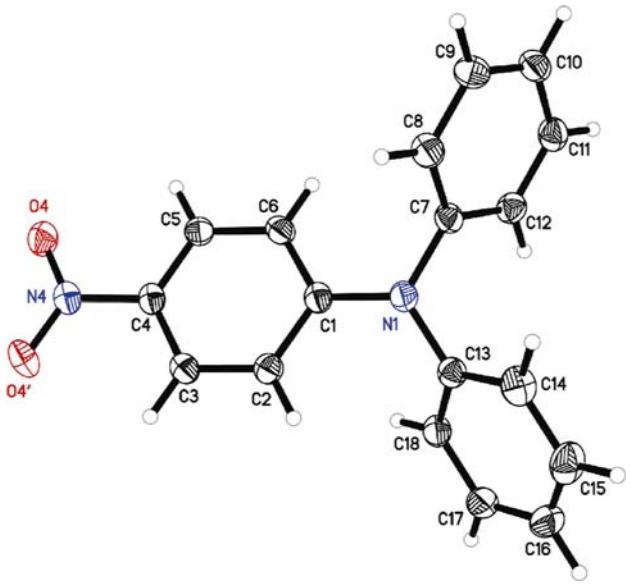

Fig. 1 Molecular structure of 4-nitrotriphenylamine. Atomic labeling scheme is based on the molecular structure determination. Displacement ellipsoids are at 50% probability level

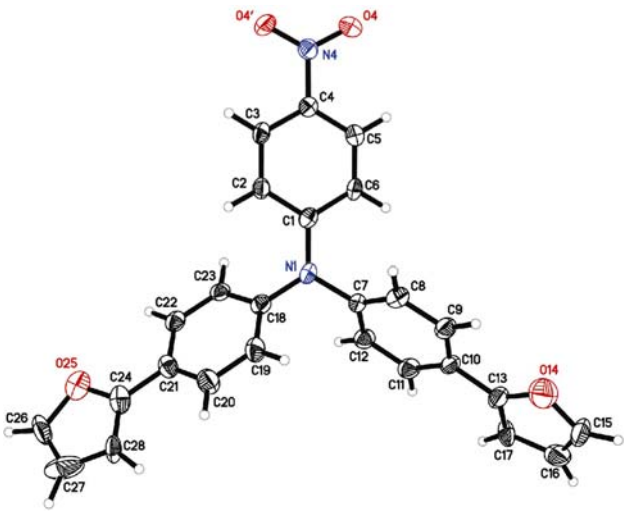

Fig. 2 Molecular structure of **3b**. Atomic labeling scheme is based on the molecular structure determination. Displacement ellipsoids are at 50% probability level

Table 1 Crystal data and structure refinement for 4-nitrotriphenylamine and **3b**

Parameters	4-nitrotriphenylamine	Monomer **3b**
Empirical formula	$C_{18}H_{14}N_2O_2$	$C_{58}H_{48}N_4O_8$
Formula weight	290.31	929.00
Temperature (K)	103(1)	103(1)
Wavelength (nm)	0.071073	0.071073
Crystal system	Orthorhombic	Triclinic
Space group	*P*bca	*P*-1
Unit cell dimensions	$a = 1.28372(10)$ nm	$a = 1.39564(6)$ nm
	$b = 1.29064(9)$ nm	$b = 1.51172(6)$ nm
	$c = 1.72640(12)$ nm	$c = 2.31004(9)$ nm
	$\alpha = \beta = \gamma = 90°$	$\alpha = 87.050(1)°$, $\beta = 89.978(1)°$, $\gamma = 76.656(1)°$
Volume (nm^3)	2.8603(4)	4.7356(3)
Z	8	4
Density (calculated) (mg/m^3)	1.348	1.303
Absorption coefficient (mm^{-1})	0.089	0.087
F(000)	1,216	1,952
Crystal size (mm^3)	$0.727 \times 0.436 \times 0.388$	$0.53 \times 0.18 \times 0.10$
Theta range for data collection	2.36–29.16°	0.88–25.35°
Index ranges	$-14 \le h \le 17$, $-13 \le k \le 17$, $-23 \le l \le 23$	$-16 \le h \le 13$, $-18 \le k \le 18$, $-27 \le l \le 27$
Reflections collected	19,292	40,296
Independent reflections	3,826 [R(int) = 0.0265]	17,217 [R(int) = 0.0421]
Completeness to $\theta = 29.16°$	98.9%	99.2%
Absorption correction	Semi-empirical from equivalents	Semi-empirical from equivalents
Max. and min. transmission	0.9552 and 0.9182	0.9910 and 0.9550
Refinement method	Full-matrix least-squares on F^2	Full-matrix least-squares on F^2
Data/restraints/parameters	3826/0/199	17217/0/1261
Goodness-of-fit on F^2	1.028	0.996
Final R indices [I > 2sigma(I)]	R1 = 0.0431, wR2 = 0.1121	R1 = 0.0621, wR2 = 0.1928
R indices (all data)	R1 = 0.0555, wR2 = 0.1211	R1 = 0.1594, wR2 = 0.2526
Largest diff. peak and hole	0.374 and −183 e nm^{-3}	0.571 and −465 e nm^{-3}

Both structures clearly show that communication of the electron-withdrawing group with the nitrogen lone pair dominates the stereoelectronics; hence, the central nitrogen adopts a near planar geometry, and there is a prominate decrease in torsion-angles for the phenyl ring bearing the electron-withdrawing substitutent in both 4-nitrotriphenylamine and **3b**. This is best illustrated by considering the dihedral angles defined by C6–C1–N1–C7 and C2–C1–N1–C18. For 4-nitrotriphenylamine the torsion-angles are 17.4(2)° and 27.1(2)°, respectively. Interestingly, the addition of the electron-rich furanyl rings at the 4,4′ positions decreases these torsion-angles to 15.6(7)° and 13.2(7)°, respectively, in **3b**. The remaining torsion-angles between the phenyl rings lacking the nitro group (e.g., C19–C18–N1–C7 and C14–C13–N1–C7) are around 55°, which is typical of triarylamines in which stereoelectronic factors are not as prevalent. For example, the torsion angles in triphenyl amines range from 30° to 56° [30–32]. For **3b** the furanyl rings are nearly coplanar with the phenyl rings showing only small torsion-angles of 9.5° and 1.6°.

Electrochemical polymerization and polymer redox behavior

Cyclic voltammograms of monomers **2** and **3** reveal an irreversible oxidation at 0.4–0.8 V versus Ag/Ag^+, Fig. 3. The differences in the anodic wave positions for the benzoyl and nitro derivatives are approximately 0.13 V. By comparison, the model compounds 4-nitrotriphenylamine and 4-benzoyltriphenylamine undergo an irreversible oxidation at 0.95 and 0.83 V, respectively, a difference of 0.12 V (Fig. 4). These oxidation potentials are consistent with those reported for other substituted triphenylamines [33]. The i_a/i_c for the voltammograms of 4-nitrotriphenylamine and 4-benzoyltriphenylamine is three indicating that the oxidation products undergo a chemical reaction.

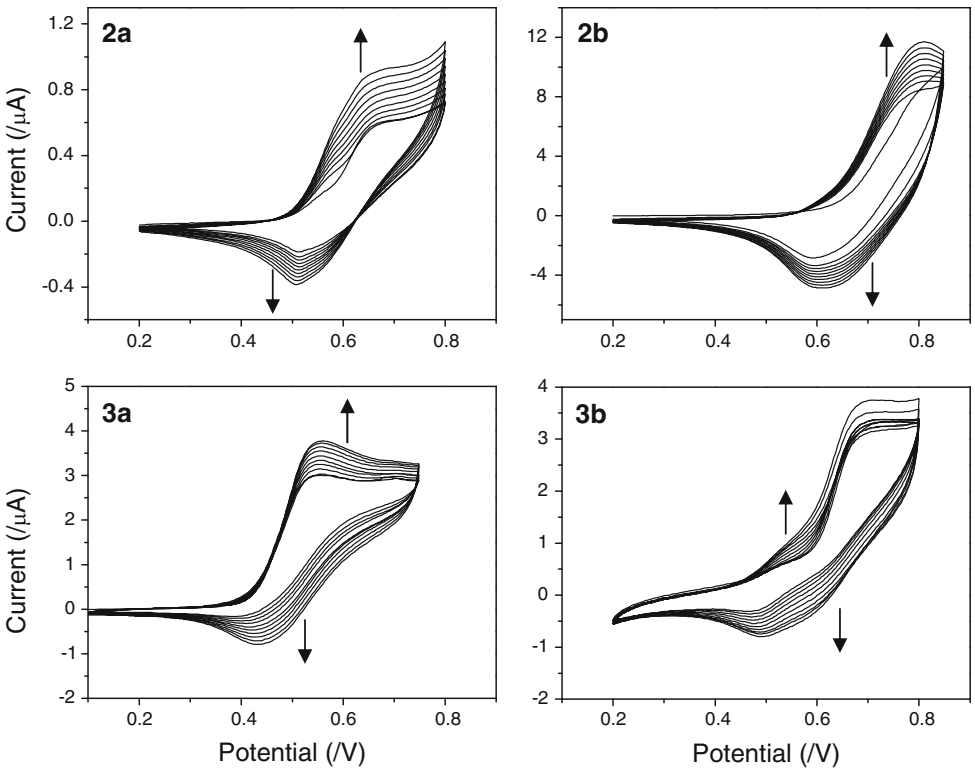

Fig. 3 Cyclic voltammograms of **2** and **3** at Pt electrodes in 0.05 M solution of monomer in acetonitrile with 0.1 M $[Bu_4N]BF_4$ electrolyte. Potentials are vs Ag/Ag^+. With each subsequent sweep additional polymer is deposited on the electrode as evident by the increasing currents

Similar nonunity i_a/i_c ratios are observed in the voltammograms of the monomers consistent with the formation of a reactive oxidation product. The increased reactivity of the radical cations $[4\text{-nitrotriphenylamine}]^+$ and $[4\text{-benzoyltriphenylamine}]^+$ compared to other triphenylamine cations is likely due to the lack of substitution at two of the 4-positions on the phenyl rings, which facilitates dimerization. The bromo derivative tris(4-bromophenyl)amine is reported to undergo a slow dimerization with the elimination of Br_2 [34]. The oxidation waves in the voltammograms likely correspond to the removal of an electron from a delocalized orbital distributed across the phenyl and heterocyclic rings rather than those localized exclusively on the furanyl or thiophenyl groups, which would require considerably higher potentials [35]. Repeated sweeping of the potential between 0 and 1 V at 50 mV/s with solutions of **2** or **3** results in the deposition of a polymer film. With each additional sweep of the potential, the oxidative and reductive currents are increased indicating the presence of a polymer film on the electrode surface. As the DFT calculations suggest, the HOMO of the radical cation $\mathbf{2b}^+$ is somewhat delocalized over the phenyl and thiophenyl rings (Fig. 5). This delocalization likely activates the carbon atom at the 5-position of the heterocycle rings that then leads to carbon–carbon bond formation and later loss of hydrogen for rearomatization. Thus, this coupling process (i.e., electrochemically induced polymerization) affords the novel hybrid polymers (Scheme 2) at the surface of the electrode.

Evidence for the polymer structures is present in the infrared spectra of the monomers, model compounds, and polymer films. The strongest absorption bands assigned to the phenyl rings (1,580 cm^{-1}) and the nitro groups (1,490 cm^{-1}, asymmetric; 1,312 cm^{-1}, symmetric) in 4-nitrotriphenyl amine and **3b** are relatively unchanged in the polymer (1,588, 1,488, and 1,318 cm^{-1}, respectively). By contrast, the bands assigned to the furanyl group at 1,511, 1,494, 1,077, and 1,008 cm^{-1} of the monomer are considerably broadened and weaker in the polymer [36, 37]. GPC analysis on chloroform extracts of poly-**3b** indicates the presence of tetramers and trimers. Presumably, the chloroform-insoluble material contains higher molecular weight polymers. Collectively, these data support the formation of the new hybrid polymers as depicted in Scheme 2.

Thin polymer films electrochemically deposited on platinum electrodes can be rinsed with clean acetonitrile without losing electrochemical activity. However, deposition of thick films (50 or more sweeps at 50 mV/s) often results in polymer films that were electrochemically inactive. Cyclic voltammetry on polymer-coated electrodes with monomer-free electrolyte reveals broad or multiple anodic waves with similarly broad return waves, Fig. 6. The electrochemical activity of the deposited films is not significantly diminished with repeated cycling (loss of less than 15% current after 10 or more cycles) as long as the potential is maintained at values less positive than 1.5 V. Potentials in excess of 1.5 V result in diminished currents

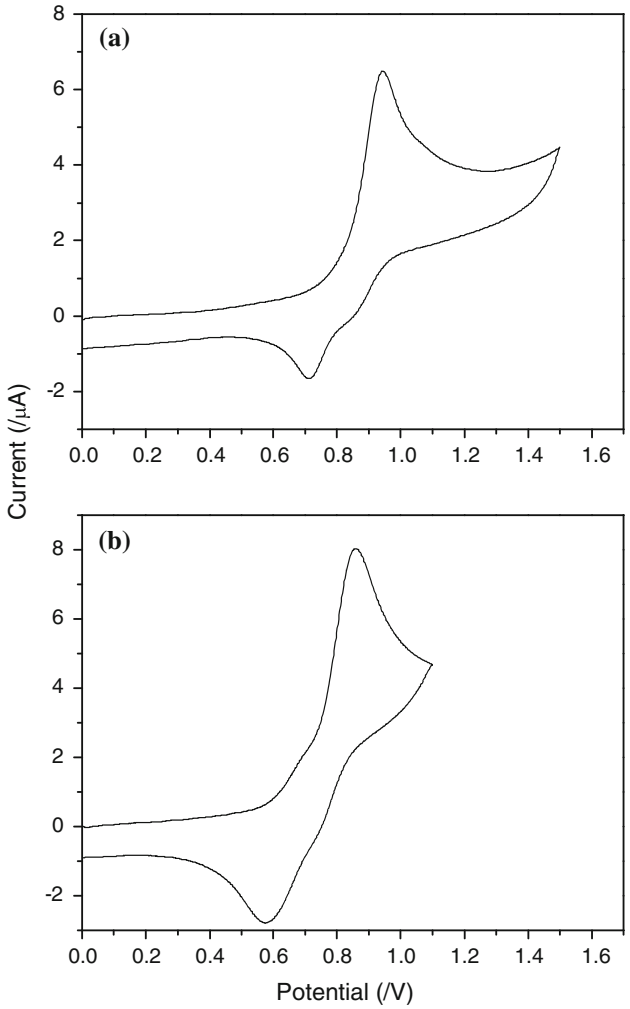

Fig. 4 Cyclic voltammograms of (**a**) 4-nitrotriphenylamine and (**b**) 4- benzoyltriphenylamine in 0.1 M $[Bu_4N]BF_4$ acetonitrile. Scan rate is 250 mV/s. Potentials are vs Ag/Ag^+

and eventual loss of electrochemical activity. Films composed of the thiophene derivatives **2** are more stable than those formed from solutions of **3**. This difference in stability likely reflects the greater reactivity of the bifuranyl unit compared to the bithiophenyl segment. Polyfuran is more susceptible to degradation by electrolyte impurities under anodic conditions compared to polythiophene [38].

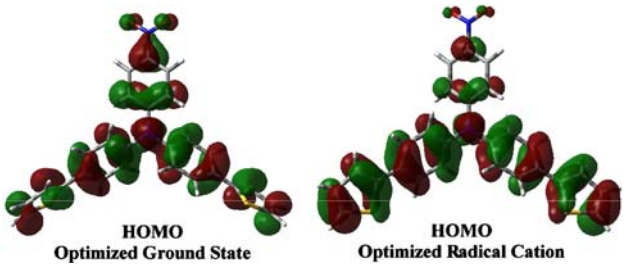

Fig. 5 HOMO of **2b** in the ground state (left) and the radical cation $\mathbf{2b}^+$ (right)

Electrochemically reversible oxidation processes in a polymer film should yield symmetric oxidation/reduction waves in the cyclic voltammogram. Voltammograms on thin films of poly-**2** and poly-**3b** are very asymmetric indicating that the redox process associated with the oxidation is electrochemically irreversible. Peak-to-peak separations for the oxidation and reduction waves are generally in excess of 100 mV. Poly-**3a** exhibits a quasi-reversible oxidation process with a peak-to-peak separation of 60 mV for the first oxidation wave. The electrochemically irreversible oxidation processes observed for films of poly-**2** and poly-**3** are similar to those reported for hybrid polymers of 4-methyltriphenylamine and arenes [20]. Not only are the oxidation/reduction peaks shifted but additional peaks and shoulders also appear without corresponding reduction or oxidation waves. These additional features suggest that the oxidation of the polymer causes a change in its chemical structure or composition. Presumably, the chemical change of the polymer causes a shift in the oxidation/reduction potential of the film. The change in the film can be due to reorganization of the polymer film, shifting of counter ions, or somehow related to counter ion motion [39, 40]. Upon reduction of the oxidized polymer, the organic film reverts to its previous chemical state. Polystyrene containing pendent dimers of triphenylamine (tetraphenylphenyldiaminobenzene) also exhibit irreversible cyclic voltametry [40]. By contrast,

Scheme 2 Polymerization process

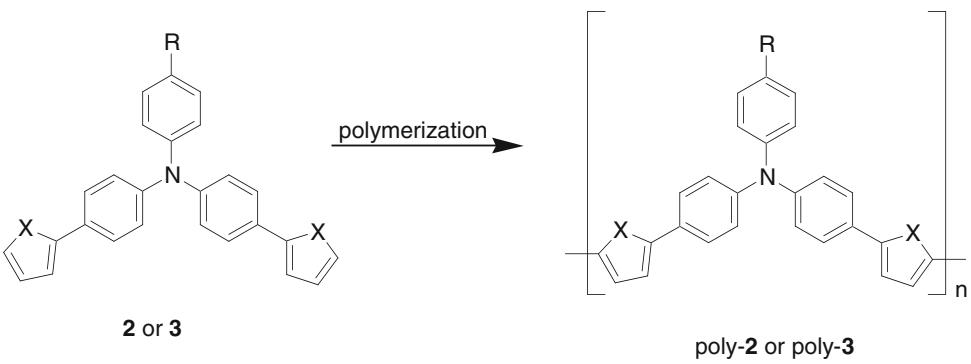

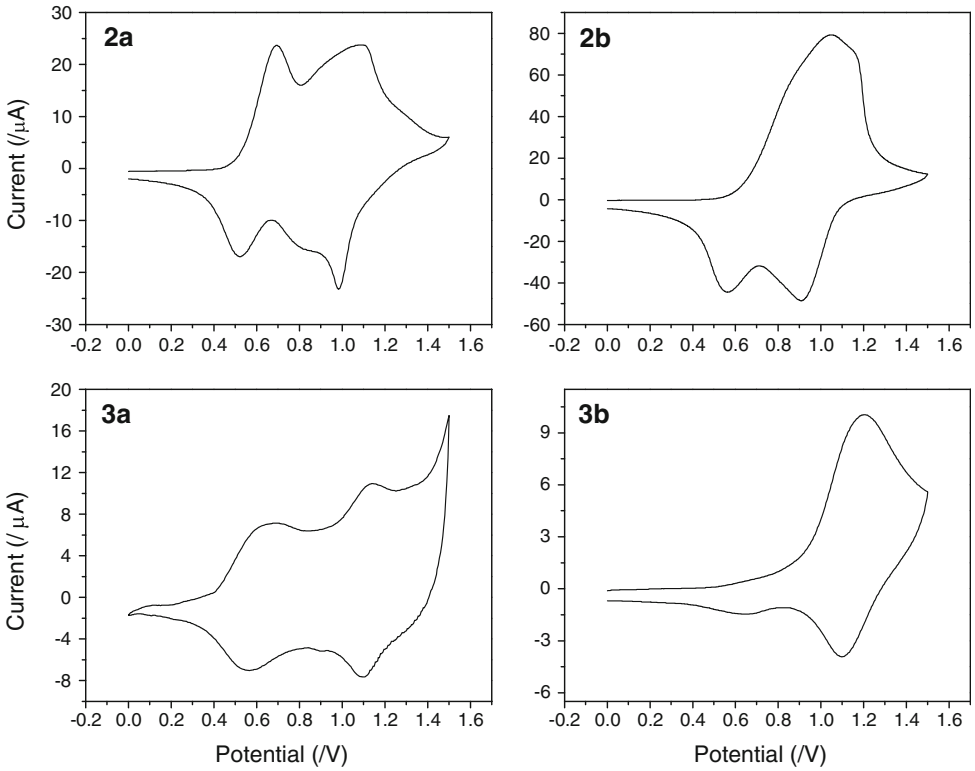

Fig. 6 Cyclic voltammograms of films of **2** and **3** electrochemically deposited on platinum disk electrodes. The electrolyte is 0.1 M $[Bu_4N]BF_4$ in CH_3CN. Potentials are vs Ag/Ag^+

solutions of poly(4-*sec*-butyltriphenylamine) produced by chemical means display more ideal redox behavior with three one-electron and completely reversible oxidation waves at 0.16, 0.41, and 0.79 V versus Ag/AgCl [41].

Importantly, these results demonstrate the electrochemical deposition of a triarylamine hybrid polymers and the formation of furan–furan and thiophene–thiophene polymer connections at relatively low potentials. Electrodeposition of polyfurans or polythiophenes from the furan or thiophene monomer requires significantly higher potentials. Under similar electrolytic conditions, furan and 2-methylthiophene are oxidized at 1.75 V and 1.5 V versus Ag/Ag^+, respectively [35]. The triarylamine functionality of **2** and **3** significantly lowers the oxidation potential of these monomers, presumably due to the extensive delocalized structure of the monomer's HOMO. These oxidation potentials can be further influenced by substitutions on the phenyl rings. However, the oxidation potentials of the resulting polymers are more difficult to predict. In these cases, the tertiary structure of the polymer and the polymer-counter anion interaction likely affect the observed oxidation waves [39]. Electroactive films of a homologous series of fluorinated poly(3-phenylthiophene) undergo quasireversible oxidation at potentials that correlate well with the sum of the Hammet parameters on the phenyl ring [42]. However, in these same systems, the reduction potentials do not correlate with the Hammet constants suggesting that ion motion plays an important role in the n-doping of these materials. To generate a series of electroactive polymers with a predicted and tunable oxidation potential requires a better understanding of the factors that determine the electronic properties of the condensed films and the relative importance of ionic motion during the doping process. Only then can the electronic structure of the polymer be finely tuned by controlling substituents on the polymer backbone and parent monomer.

DFT calculations of monomer and polymer model structures

The standard oxidation potential for **2b** and **3b** and the model acetyl compounds bis-(4-heterocyclic-2-yl-phenyl)-(4-acetyl-phenyl-amine) were calculated using the method of Liu and Guo [43]. For comparison, calculations on the acetyl compounds are approximates for the benzoyl monomers. Solvation energies were ignored since only the relative differences were needed and the compounds are reasonably expected to have similar solvation energies depending on the oxidation state of the molecule. The calculated oxidation potentials of the furanyl derivatives are slightly lower than the calculated values for the thiophene analogues in agreement with the literature [44] (Table 2). However, the spread in calculated oxidation potentials (0.53–0.74 V) is rather large considering that both the acetyl and nitro groups would shift the oxidation potential in similar directions relative to the parent phenyl

Table 2 Calculated ionization and oxidation potentials for select triarylamines and bis-(4-heterocyclic-2-yl-phenyl)-aryl-amines

Compound	Vert IP (eV)	Adiabatic IP (eV)	Corr IP[a] (eV)	E^0 (V)
Nitrotriphenylamine	7.27	7.16	7.44	1.22
Acetyltriphenylamine	6.94	6.87	7.15	0.98
2b, R = NO_2	6.76	6.57	6.85	0.74
3b, R = NO_2	6.65	6.53	6.81	0.70
X = S, R = acetyl	6.51	6.37	6.65	0.57
X = O, R = acetyl	6.41	6.32	6.60	0.53

[a] Corrected IP (calc IP + 0.28 eV) and E^0 (corr IP x 0.82 – 4.88, versus NHE) were calculated by the method in Yao Fu et al. [43]

compound. In addition, the large variation in calculated oxidation potentials suggests that the electronic effects of the nitro and acetyl groups are directly influencing the HOMO energies. Molecular orbital diagrams of **2b** indicate that the HOMO is distributed over all five rings including the pendent 4-nitrophenyl substituent (Fig. 5). Participation of the pendent phenyl ring in the HOMO structure suggests that the electronic properties of the monomer and polymer may be controlled through chemical manipulations at these positions. A DFT calculation on a relaxed oligomer indicates a similar distribution of the HOMO across the conjugated ring systems with some participation by the pendent phenyl rings (Fig. 7). Unfortunately, formal oxidation potential could not be obtained by cyclic voltammetry due to the irreversible nature of the oxidation/polymerization process, vida supra. However, the trend in the calculated oxidation potentials for **2b** and **3b** and the acetyl derivatives correlates with the experimental potentials for the onset of oxidation as determined from cyclic voltammetry (Fig. 3 and Table 2). The onset of polymerization is calculated as the potential where the oxidation current is half i_{max} for the first cycle. While altering the chemical functionality of the pendent side groups may provide some control over the oxidation potentials for polymerization, controlling the electrochemical properties of the resulting polymer is significantly more challenging and requires considerations of polymer–ion interactions and polymer reorganizations.

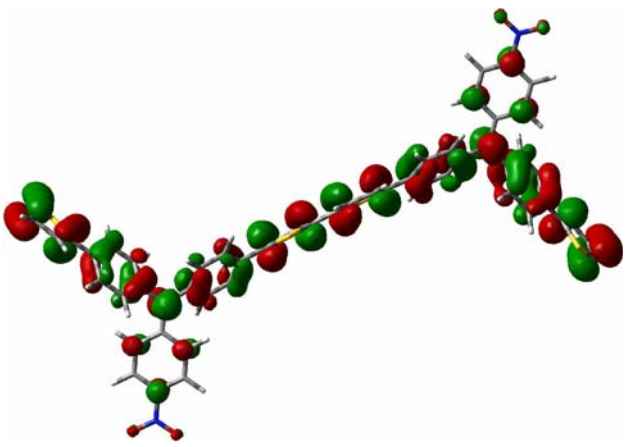

Fig. 7 HOMO of relaxed oligomer of poly-**2b**

Conclusion

Novel poly(thiophenylanilino) and poly(furanylanilino) polymers were electrochemically synthesized from the monomers **2** and **3**. The polymerization potential of the monomers is consistent with DFT calculations suggesting that the oxidation potentials can be chemically tuned by altering the pendent functional groups on the triaryl amine. Unfortunately, the oxidation potentials of the polymers did not demonstrate the same correlation suggesting that other factors influence the redox properties of the organic film rather than just the pendent side groups. When constructing electronic devices such as polymer supercapacitors, the redox properties of the polymer are unlikely to be as predictable as those of the parent monomer. The importance of the polymer structure, reorganization, and polymer–ion interaction will likely need to be considered as well. Only by understanding all the contributing factors can one assemble a redox active polymer/electrolyte system with predictable charging and discharging properties. The charging and discharging properties of the new polymers are currently being investigated for applications in organic supercapacitors.

Acknowledgement NP thanks the Strategic Environmental Research and Development Program for support.

References

1. Chollet P-A (1987) Rev Phys Appl 22:1221
2. Nalwa HS (1993) Adv Mater 5:341. doi:10.1002/adma.19930050504
3. Choi KS, Kwak JG, Lee CH, Kim H, Char KH, Kim DY, Zentel R (2008) Poly Bull 59:795. doi:10.1007/s00289-007-0815-4
4. Dimitrakopoulos CD, Malenfant PRL (2002) Adv Mater 14:99. doi:10.1002/1521-4095(20020116)14:2<99::AID-ADMA99>3.0.CO;2-9
5. Sim JH, Yamada K, Lee SH, Nokokura S, Sato H (2007) Syn Met 157:940. doi:10.1016/j.synthmet.2007.09.009
6. Chahma M, Gilroy JB, Hicks RG (2007) J Mater Chem 17:4768. doi:10.1039/b711693d
7. MacDiarmid AG, Mu SL, Somasiri MLD, Wu W (1985) Mol Cryst Liq Cryst 121:187. doi:10.1080/00268948508074859
8. Kitani A, Kaya M, Sasaki K (1986) J Electrochem Soc 133:1069. doi:10.1149/1.2108787
9. Ghosh S, Inganäs O (1999) Adv Mater 11:1214. doi:10.1002/(SICI)1521-4095(199910)11:14<1214::AID-ADMA1214>3.0.CO;2-3

10. Kalaji M, Murphy PJ, Williams GO (1999) Syn Met 102:1360. doi:10.1016/S0379-6779(98)01334-4
11. Arbizzani C, Mastragostino M, Soavi F (2001) J Power Sources 100:164. doi:10.1016/S0378-7753(01)00892-8
12. Fusalba F, Ho HA, Breau L, Bélanger D (2000) Chem Mater 12:2581. doi:10.1021/cm000011r
13. Strohriegl P, Grzulevicius JV (2002) Adv Mater 14:1439. doi:10.1002/1521-4095(20021016)14:20<1439::AID-ADMA1439>3.0.CO;2-H
14. Wang H, Ryu JT, Kim DU, Han YS, Park LS, Cho HY, Lee SJ, Kwon Y (2007) Mol Cryst Liq Cryst 471: 279. doi:10.1080/15421400701548506
15. Sicot L, Geffroy B, Lorin A, Raimond P, Sentein C, Nunzi J-M (2001) J Appl Phys 90:1047. doi:10.1063/1.1378064
16. Yoshino K, Tada K, Fujii A, Conwell EM, Zakhidov AA (1997) IEEE Trans Electron Dev 44:1315. doi:10.1109/16.605474
17. Shirota Y (2000) J Mater Chem 10:1. doi:10.1039/a908130e
18. Ishikawa M, Kawai M, Ohsawa Y (1991) Syn Met 40:231. doi:10.1016/0379-6779(91)91778-9
19. McKeown NB, Badriya S, Helliwell M, Shkunov M (2007) J Mater Chem 17:2088. doi:10.1039/b614235d
20. Strzelec K, Fugino N, Ha J, Ogino K, Sato H (2002) Macromol Chem Phys 203:2488. doi:10.1002/macp.200290031
21. Bellmann E, Shaheen SE, Thayumanavan S, Barlow S, Grubbs RH, Marder SR, Kippelen B, Peyghambarian N (1998) Chem Mater 10:1668. doi:10.1021/cm980030p
22. Feigenbaum WM, Michel RH (1971) J Poly Sci Part A-1: Poly Chem 9:817. doi:10.1002/pol.1971.150090322
23. Eberson L, Hartshorn MP, Svensson JO (1997) Acta Chem Scand 51:279
24. Gaussian 03, Revision D.01, Frisch MJ, Trucks GW, Schlegel HB, Scuseria GE, Robb MA, Cheeseman JR, Montgomery JA Jr, Vreven T, Kudin KN, Burant JC, Millam JM, Iyengar SS, Tomasi J, Barone V, Mennucci B, Cossi M, Scalmani G, Rega N, Petersson GA, Nakatsuji H, Hada M, Ehara M, Toyota K, Fukuda R, Hasegawa J, Ishida M, Nakajima T, Honda Y, Kitao O, Nakai H, Klene M, Li X, Knox JE, Hratchian HP, Cross JB, Bakken V, Adamo C, Jaramillo J, Gomperts R, Stratmann RE, Yazyev O, Austin AJ, Cammi R, Pomelli C, Ochterski JW, Ayala PY, Morokuma K, Voth GA, Salvador P, Dannenberg JJ, Zakrzewski VG, Dapprich S, Daniels AD, Strain MC, Farkas O, Malick DK, Rabuck AD, Raghavachari K, Foresman JB, Ortiz JV, Cui Q, Baboul AG, Clifford S, Cioslowski J, Stefanov BB, Liu G, Liashenko A, Piskorz P, Komaromi I, Martin RL, Fox DJ, Keith T, Al-Laham MA, Peng CY, Nanayakkara A, Challacombe M, Gill PMW, Johnson B, Chen W, Wong MW, Gonzalez C, Pople JA (2004) Gaussian, Inc., Wallingford, CT
25. Wright ME, Jin M-J (1989) J Org Chem 54:965. doi:10.1021/jo00265a043
26. Hassan J, Sevignon M, Gozzi C, Schulz E, Lemaire M (2002) Chem Rev 102:1359. doi:10.1021/cr000664r
27. Stille JK (1986) Angew Chem Int Ed Engl 25:508. doi:10.1002/anie.198605081
28. Hoshino M, Degenkolb P, Curran DP (1997) J Org Chem 62: 8341. doi:10.1021/jo9709413
29. Brody MS, Finn MG (1999) Tetrahedron 40:415. doi:10.1016/S0040-4039(98)02384-3
30. Sobolev AN, Belsky VK, Romm IP, Chernikova NY (1985) Acta Crysta Sect C 41:967. doi:10.1107/S0108270185006217
31. Kongrev DV, Kovalevsky AY, Litvinov AL, Drichko NV, Tarasov BP, Coppens P, Lyubovskaya RN (2002) J Solid State Chem 168:474. doi:10.1006/jssc.2002.9732
32. Manifor T, Rohani S, Jennings MS (2004) Acta Cryst Sect E 60:o2301. doi:10.1107/S1600536804028247
33. Stechan E (1987) Top Curr Chem 147:1
34. Eberson L, Larsson B (1986) Acta Chem Scand Ser B 40:210
35. Demirboğa B, ÖNal AM (1999) Syn Met 99:237. doi:10.1016/S0379-6779(98)01509-4
36. Wan X, Yan F, Jin S, Liu X, Xue G (1999) Chem Mater 11:2400. doi:10.1021/cm9900453
37. Gök A, Sari B, Talu M (2005) J Appl Poly Sci 98: 2440. doi:10.1002/app.22439
38. Wan X-B, Li LHJ-B, Zhou D-S, Xue G, Wang T-W (2002) J Appl Poly Sci 86:3160. doi:10.1002/app.11343
39. Zotti G, Schiavon G, Zecchin S (1995) Syn Met 72:275. doi:10.1016/0379-6779(95)03280-0
40. Son JM, Sakaki Y, Ogino K, Sato H (1997) IEEE Trans Electron Dev 44:1307. doi:10.1109/16.605473
41. Goodson FE, Hauck SI, Hartwig JF (1999) J Am Chem Soc 121:7527. doi:10.1021/ja990632p
42. Laforgue A, Simon P, Fauvarque J-F (2001) Syn Met 123:311. doi:10.1016/S0379-6779(01)00296-X
43. Fu Y, Lie L, Yu H-Z, Wang Y-M, Guo Q-X (2005) J Am Chem Soc 127:7227. doi:10.1021/ja0421856
44. Miyata Y, Nishinaga T, Komatsu K (2005) J Org Chem 70: 1147. doi:10.1021/jo048282z